

## Article (refereed)

---

**Lofts, Stephen; Tipping, Edward.** 2011 Assessing WHAM/Model VII against field measurements of free metal ion concentrations: model performance and the role of uncertainty in parameters and inputs. *Environmental Chemistry*, 8 (5). 501-516. [10.1071/EN11049](https://doi.org/10.1071/EN11049)

This version available <http://nora.nerc.ac.uk/15323/>

NERC has developed NORA to enable users to access research outputs wholly or partially funded by NERC. Copyright and other rights for material on this site are retained by the authors and/or other rights owners. Users should read the terms and conditions of use of this material at <http://nora.nerc.ac.uk/policies.html#access>

**This document is the author's final manuscript version of the journal article, incorporating any revisions agreed during the peer review process. Some differences between this and the publisher's version remain. You are advised to consult the publisher's version if you wish to cite from this article.**

The definitive version is available at [www.publish.csiro.au/](http://www.publish.csiro.au/)

Contact CEH NORA team at  
[noraceh@ceh.ac.uk](mailto:noraceh@ceh.ac.uk)

1 **Research Paper (GEOSPEC Special Issue)**

2 **Assessing WHAM/Model VII against field measurements of free metal ion**  
3 **concentrations: model performance and the role of uncertainty in parameters and**  
4 **inputs**

5 *Stephen Lofts<sup>A,B</sup> and Edward Tipping<sup>A</sup>*

6 <sup>A</sup>Centre for Ecology and Hydrology, Lancaster Environment Centre, Library Avenue, Bailrigg,  
7 Lancaster, LA1 4AP, UK.

8 <sup>B</sup>Corresponding author. Email: stlo@ceh.ac.uk

9 **Environmental context.** The chemical speciation of metals in waters is of great importance in determining  
10 their transport, fate and effects in the environment. Modelling chemical speciation is valuable for making  
11 predictions about these effects. Here a model of metal speciation is tested against field data, and  
12 recommendations are made as to how both model and measurements might be improved in future.

13 **Abstract** A key question in the evaluation of chemical speciation models is: how well do model predictions  
14 compare against speciation measurements? To address this issue, the performance of WHAM/Model VII in  
15 predicting free metal ion concentrations in field samples has been evaluated. A statistical sampling method  
16 considering uncertainties in input measurements, model parameters and the binding activity of dissolved organic  
17 matter was used to generate distributions of predicted free ion concentrations. Model performance varied with  
18 the metal considered and the analytical technique used to measure the free ion. Generally, the best agreement  
19 between observation and prediction was seen for aluminium, cobalt, nickel, zinc and cadmium. Important  
20 differences in agreement between model and observations were seen, depending upon the analytical technique.  
21 In particular, concentrations of free ion determined with voltammetric techniques were largely over-predicted by  
22 the model. Uncertainties in model predictions varied among metals. Only for aluminium could discrepancies  
23 between observation and model could be explained by uncertainties in input measurements and model  
24 parameters. For the other metals, the ranges of model predictions were mostly too small to explain the  
25 discrepancies between model and observation. Incorporating the effects of uncertainty into speciation model  
26 predictions allows for more rigorous assessment of model performance.

27 EN11049

28 S. Lofts and E. Tipping

29 Running header: Chemical speciation model testing

30 **Introduction**

31 The modelling of equilibrium metal speciation in natural waters has assumed an increasing  
32 importance in recent years as the role of speciation in metal bioavailability and toxicity has been  
33 recognised. Advances in the understanding of the chemistry of natural components of waters,  
34 particularly organic matter (humic substances), have allowed the development of sophisticated metal–  
35 humic binding models, such as NICA–Donnan<sup>[1]</sup> and Humic Ion-Binding Model VI.<sup>[2]</sup> A predecessor

36 to Model VI, Model V,<sup>[3]</sup> is incorporated into the Biotic Ligand Model<sup>[4]</sup> of metal bioavailability. The  
37 evaluation of the performance of these models against field speciation data is thus becoming a  
38 research area of great importance. These models simulate the binding of protons and metal ions to  
39 humic substances (humic and fulvic acids), which are generally thought to be the dominant form of  
40 non-living organic matter in terrestrial and aquatic environments, and which are known to bind some  
41 metals strongly. The models are parameterised against laboratory data on the binding of protons and  
42 metals to isolated samples of humic substances, and thus their application to field data rests on the  
43 important assumption that the ion-binding properties of dissolved organic matter in the field are  
44 similar to those of isolated humics.

45 There are two key research questions when evaluating the performance of chemical speciation  
46 models:

- 47 1. How well do model predictions compare against speciation measurements on field samples?
- 48 2. How does uncertainty in model parameters and input variables influence the distribution of model  
49 predictions?

50 Evaluating model predictions of solid–solution metal partitioning in surface waters is fairly  
51 straightforward<sup>[5]</sup> as the separation of solid and solution phases can be readily done (e.g. by filtration).  
52 However, evaluation of speciation within the dissolved phase, which is important for bioavailability  
53 models, is more complex as field measurements of dissolved metal speciation are required. In recent  
54 years several techniques have been developed for measuring free metal ions in surface waters at  
55 environmental concentrations, such as the Donnan membrane technique (DMT),<sup>[6]</sup> a range of  
56 voltammetric techniques<sup>[7–13]</sup> and ion-exchange methods,<sup>[14]</sup> and there is a growing body of measured  
57 free metal ion concentration data. Several studies<sup>[7,15–18]</sup> have compared speciation calculations of free  
58 metal ion concentrations against measurements made by a variety of methods, however, to date there  
59 has been no systematic attempt to synthesise and model the data as a single exercise.

60 In assessing the ability of a humic ion-binding model to predict measured free ion concentrations in  
61 the field four factors must be considered:

- 62 • the degree to which the binding properties of isolated humic substances in the laboratory reflect  
63 the binding properties of dissolved organic matter (DOM) in the field;
- 64 • uncertainties in key input variables, such as pH, dissolved organic carbon (DOC) nature and  
65 concentration, dissolved metal and other solute concentrations, required by the model;
- 66 • uncertainties in the model parameters; and
- 67 • uncertainty in measured concentrations of free metal ions in the field.

68 The first factor is the most challenging to assess, as a thorough analysis would entail a  
69 comprehensive characterisation of field DOM, including the ion-binding properties of the humic

70 component. Therefore, past modelling efforts have taken a pragmatic approach whereby a portion of  
71 the measured DOM is assumed to have the ion-binding properties of humic acid, fulvic acid (FA), or a  
72 mixture of both,<sup>[6,19]</sup> reflecting the apparent ‘binding activity’ of the DOM. Using this approach, a  
73 ‘best average’ binding activity, based on the apparent binding activity of DOM from a range of field  
74 samples, has been derived.<sup>[19]</sup> The concentration of humic substances required to simulate free Al and  
75 Cu concentrations in freshwater samples is similar to, but on average somewhat lower than, the  
76 concentration of DOM.<sup>[19,20]</sup> The average DOM ‘activity’ is similar for separate studies involving Al  
77 and Cu, and so in the absence of similar data for the other metals it is reasonable to apply the same  
78 average ‘activity’ in studies involving speciation of the latter. This supports the hypothesis that the  
79 ion-binding properties of natural organic matter are similar to those of isolated humic substances.  
80 However, the optimal binding activity has also been shown to vary among field samples and thus  
81 represents a source of uncertainty if a ‘best average’ value is used for predictive work. For example,  
82 Kalis and coworkers<sup>[6]</sup> studied how varying the proportions of HA and FA comprising DOM  
83 influenced the prediction of the free ion by the NICA–Donnan model, and found that for copper the  
84 free ion prediction varied by four orders of magnitude, whereas for nickel, zinc, cadmium and lead the  
85 variation was up to an order of magnitude.

86 The effects on predictions of uncertainties in input variables and model parameters are amenable to  
87 analysis, provided suitable uncertainty ranges can be defined. Uncertainty in input variables arises  
88 from measurement error, and is present in all measurements used as inputs to the model. As the input  
89 data for a speciation problem will comprise multiple measurements including pH, temperature, and  
90 concentrations of major ions, dissolved organic carbon and metal, multiple sources of input variable  
91 uncertainty exist. Uncertainty in model parameters arises because the humic-binding models are  
92 parameterised using multiple datasets (where available) for metal binding to isolated humic  
93 substances, with the aim of producing ‘best average’ binding parameters. Parameterisation to multiple  
94 laboratory datasets gives multiple fitted values of the metal–humic binding constant which will  
95 exhibit a degree of variability, giving rise to uncertainties in the ‘best average’ values.

96 Little research has been done into the influences of uncertainty on the predictions of chemical  
97 speciation models, although methods for doing so have been presented (e.g. Anderson<sup>[21]</sup>). Given the  
98 complexity of speciation calculations, statistical sampling approaches (e.g. Monte Carlo analysis)  
99 have proved most popular in application (e.g. Groenenberg et al.<sup>[22]</sup>). Such approaches involve the  
100 generation of a sample set of an input or a parameter, by repeated sampling from a presumed  
101 statistical distribution of values, and the generation of a sample set of model outputs from these  
102 sample input sets. An advantage of this approach is that multiple sample sets, representing  
103 uncertainties in more than one input and/or parameter, may be simultaneously generated in order to  
104 study the combined effect on the distribution of model outputs.

105 Incorporating the ability to assess uncertainties into chemical speciation models would allow users  
106 to assess the main sources of uncertainty in their predictions, and would highlight those uncertainties  
107 to which the models are most sensitive, allowing focusing of future research efforts. The development  
108 of Humic Ion Binding Model VII<sup>[23]</sup> and the parallel development of an updated version of the  
109 WHAM model, has afforded the opportunity to extend WHAM to allow uncertainty assessments on  
110 calculations to be performed. In this paper we present the results of a comprehensive study of the  
111 performance of the newly updated WHAM, which we term WHAM/Model VII. We have collated  
112 available measurements of free metal ion concentrations in freshwaters along with associated  
113 measurements of pH, major ions and DOC where these are available. Uncertainty in the model  
114 predictions has been quantified using a Monte Carlo approach with uncertainties represented by  
115 distributions of selected model parameters and water quality input variables. Free ion measurements  
116 and model predictions are compared on the basis of goodness-of-fit and bias. Deviations between  
117 measurement and modelled outputs are assessed against the predicted ranges of variability in the free  
118 metal ion concentrations arising from the uncertainties considered.

## 119 **Methods**

120 A glossary of parameters and terms used herein is provided in the ‘Glossary of terms and parameters  
121 used in this study’ section.

### 122 *WHAM/Model VII*

123 Humic Ion-Binding Model VII<sup>[23]</sup> describes ion (proton and cationic metal) binding to HA and FA  
124 using a structured formulation of discrete binding site types to describe heterogeneity in ion binding  
125 strengths. The formulation of binding site types, and their interrelationships, in terms of relative  
126 abundances and binding strengths for protons and other cations, is done with the goal of adequately  
127 describing the binding of protons and cations to isolated HAs and FAs in laboratory studies using the  
128 minimum necessary set of parameters. Proton binding is simulated using the equilibrium:



130 where R represents a binding site. Eight sites are defined: four strong acid (Type A) with a total  
131 density of  $n_A$  moles per gram, and four weak acid (Type B) with a total density of  $n_B$  moles per gram.  
132 The total density of the B sites ( $n_B$ ) is fixed to half the density of the A sites ( $n_A$ ). Each of the Type A  
133 sites has the same density (i.e.  $n_A/4$ ) and each Type B site also has the same density (i.e.  $n_B/4$ ). The  
134 intrinsic proton binding strength to each site type is defined by a central  $pK_{A/B}$  value and a spread  
135 factor,  $\Delta pK_{A/B}$ .

136 Metal binding equilibria are defined as follows:

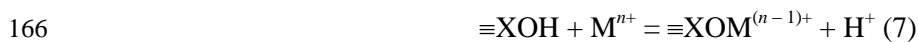


139 
$$R_{\text{tri}}^{3-} + M^{z+} = RM^{(z-3)+} \quad (4)$$

140 where  $R_{\text{mon}}$ ,  $R_{\text{bi}}$  and  $R_{\text{tri}}$  represent monodentate, bidentate and tridentate binding sites. There are two  
 141 intrinsic binding constants per metal,  $\log K_{\text{MA}}$  and  $\log K_{\text{MB}}$ , referring to monodentate binding to the  
 142 Type A and Type B sites. The relationship between  $\log K_{\text{MA}}$  and  $\log K_{\text{MB}}$  for each metal is fixed, so  
 143 only  $\log K_{\text{MA}}$  needs to be fitted. Bidentate and tridentate metal binding sites are generated by  
 144 calculating the proportions of single sites that are able to form pairs and triplets, assuming a spherical  
 145 shape for the humic molecules. Metal binding strengths are calculated by summing the  $\log K_{\text{MA/MB}}$   
 146 values for the individual sites. Additional heterogeneity of binding strength is achieved by an  
 147 additional metal-specific parameter ( $\Delta LK_2$ ) that is used to increase the binding strength of subsets of  
 148 the bidentate and tridentate sites. A total of 9 % of the bidentate sites have the logarithms of their  
 149 binding strength increased by  $\Delta LK_2$  and 0.9 % have increases of  $2\Delta LK_2$ . For tridentate sites the  
 150 respective increases are  $1.5\Delta LK_2$  and  $3\Delta LK_2$ .

151 The intrinsic proton and metal binding constants  $pK_{\text{A/B}}$  and  $\log K_{\text{MA/MB}}$  are defined for a state of  
 152 zero electrical charge of the humic substances. Development of charge, by ion binding and release,  
 153 modifies the overall binding strengths because of attractive or repulsive electrostatic forces between  
 154 the humic molecules and the binding ions. This effect is taken into account by empirical electrostatic  
 155 terms that modify the intrinsic binding constants. Counterion accumulation adjacent to humic  
 156 molecules is simulated by a Donnan model.

157 Besides Model VII, the WHAM code comprises submodels for ion binding to metal oxides<sup>[24]</sup> and a  
 158 cation exchanger, and solution speciation. Ion binding to metal oxides is described using a surface  
 159 complexation model. As with Model VII, relationships among binding site densities, and binding  
 160 strengths, are fixed where this facilitates an adequate description of metal binding to oxides under  
 161 laboratory conditions with a minimal parameter set. Proton and metal binding reactions are described  
 162 using the following equilibria, where  $\equiv\text{XOH}$  represents a surface hydroxy group, X being an atom of  
 163 the metal comprising the metal oxide:



167 for which the intrinsic binding constants are described respectively by parameters  $K_{1,\text{oxide}}$ ,  $K_{2,\text{oxide}}$  and  
 168  $K_{\text{MH,oxide}}$ . The surface sites are assumed to be homogeneous with respect to proton binding.  
 169 Heterogeneity in metal binding is achieved using the expression

170 
$$pK_{\text{MH,oxide},y} = pK_{\text{MH,oxide},y} + \Delta pK_{\text{MH,oxide}}$$

171 where  $y = 0$  for 90.1 % of the sites,  $y = 1$  for 9 % of the sites and  $y = 2$  for 0.9 % of the sites. The term  
 172  $\Delta pK_{\text{MH,oxide}}$  is a binding strength heterogeneity term specific to the oxide but common to all metals.

173 Four types of metal oxide are simulated: iron(III) oxide, aluminium oxide, manganese oxide and  
174 silica.

175 Electrostatic effects on binding strength are described by empirical electrostatic terms and  
176 counterion accumulation adjacent to the mineral surface is simulated by a Donnan model. The cation  
177 exchanger is defined by a fixed (negative) surface charge per unit mass. Cation binding by  
178 electrostatic accumulation is described by a Donnan model.

179 Equilibria among simple ions in solution are described by conventional mole balance equations.  
180 The precipitation of aluminium and iron(III) hydroxides is simulated by conventional solubility  
181 products. Alternatively, the solution chemistry of aluminium and iron(III) may be simulated by  
182 assuming equilibrium with the hydroxide. Here we use the previously quoted standard solubility  
183 product of 8.5 and enthalpy of  $-107 \text{ kJ mol}^{-1}$  for aluminium(III) hydroxide.<sup>[25]</sup> A solubility product  
184 expression for iron(III) hydroxide was derived by Lofts and co-workers<sup>[26]</sup> using WHAM/Model  
185 VI. We have updated these calculations using WHAM/Model VII (see Accessory publication for  
186 details). An enthalpy of iron(III) hydroxide solubility of  $-100.4 \text{ kJ mol}^{-1}$ <sup>[27]</sup> was used. The model  
187 allows iron(III) and aluminium(III) hydroxide precipitates to have chemically active surfaces, which  
188 are simulated using the surface complexation model.

189 WHAM/Model VII may be used to simulate partitioning of metals between the particulate and  
190 solution phases in a freshwater, by specifying concentrations of chemically active substances (humic  
191 and FAs, metal oxides, cation exchanger) in the particulate phase. Concentrations of any of these  
192 binding substances may also be specified to be present in the solution phase (concentrations of these  
193 substances in the solution phase are defined as ‘colloidal’ in WHAM/Model VII). As WHAM/Model  
194 VII is a purely chemical model, the method used to distinguish the particulate and solution phases  
195 (e.g. filter size used to isolate particulate matter from the solution) is not important. Alternatively, the  
196 model may be used to simulate speciation in the filtrate phase alone, as is done in this study.

#### 197 *Consideration of uncertainty in WHAM/Model VII*

198 To produce estimates of uncertainty in model output, WHAM/Model VII has been developed to allow  
199 uncertainty in parameters and measurements to be inputted and for measures of the resulting  
200 uncertainty to be outputted. Output uncertainties are calculated using a Monte Carlo method. Each  
201 input,  $x_i$  (parameter or input variable), for which uncertainty is to be considered, is assigned an  
202 absolute or relative uncertainty factor ( $\sigma_i$  or  $p_i$ ). Sample sets of  $y$  values of each variable are then  
203 generated by random sampling. A perturbation factor  $q$ , generated by random sampling from a  
204 standard normal distribution, is used to calculate perturbed values of each variable. For variables  
205 assigned an absolute uncertainty the perturbed value is given by:

$$206 \quad x'_{i,j} = x_i + q \cdot \sigma_i \quad (1)$$

207 For variables assigned a relative uncertainty the perturbed value is given by<sup>[24]</sup>:

$$208 \quad x'_{i,j} = \exp \ln x_i + q \cdot \sqrt{\ln 1 + p_i} \quad (2)$$

209 such that for each variable a sample set of values  $x_{i,1}, x_{i,2}, x_{i,3}, \dots, x_{i,y}$  is generated. The model is run  $y$   
210 times, each run using one set of the sampled variables, producing for each output a population of  
211 values. A further run is done using the unperturbed set of inputs, to produce a baseline prediction. The  
212 advantages of using a Monte Carlo approach include the rapid and robust generation of many  
213 ‘scenarios’ (samples) by statistical sampling from parameter and input variable distributions, and the  
214 ability to impose different distributions of uncertainty on different input variables and parameters.  
215 When uncertainty in humic–metal binding strengths ( $\log K_{MA}$ ) is considered, a single perturbation  
216 factor  $q$  is applied per sample, so that the metal binding strengths are always all perturbed in the same  
217 direction and by the same proportion of their uncertainty factors. For metals having the same  
218 uncertainty factor the relative values of their  $\log K_{MA}$  values are thus kept the same. This is done  
219 because we consider it reasonable to assume that the molecular variability in humic substances giving  
220 rise to variability in metal binding strengths is likely to affect the binding of all metals to a similar  
221 degree and in the same direction. The same restriction is also applied when calculating uncertainties  
222 in the parameter  $pK_{MH,oxide}$  for metal binding to oxides.

223 Variability in the predicted free ion concentrations in theoretical calculations and modelling of  
224 measured free metal ions was quantified by calculating the 16–84 % interquartile range of predicted  
225  $\log$  free ion concentration ( $Q_{16-84}$ ). The 2.5–97.5 % interquartile range ( $Q_{2.5-97.5}$ ) was used to assess the  
226 importance of the variability in outputs in relation to the observations, and thus the overall role of  
227 uncertainty in explaining the discrepancies between observation and prediction. If the observed free  
228 ion concentration falls within this interquartile range there is at least a 95 % probability that the  
229 discrepancy between observation and prediction can be attributed to the uncertainties used to generate  
230 the spread of outputs. The  $Q_{16-84}$  and  $Q_{2.5-97.5}$  interquartile ranges are approximately equivalent to  $\pm 1$  or  
231  $\pm 2$  standard deviations respectively around the mean of a normally distributed variable. Using these  
232 ranges, rather than calculating the standard deviation of the output, takes into account any deviation  
233 from normality of the output distribution, while providing a measure of the distribution that is  
234 consistent with the concept of the standard deviation as it applies to normally distributed data.

### 235 *Speciation and uncertainty calculations*

236 The speciation modelling presented in this study comprises theoretical calculations of dissolved metal  
237 speciation, including free metal ion concentrations, in field samples in which the free metal ion  
238 concentration has been measured. Theoretical uncertainty calculations were done to allow a  
239 systematic analysis and understanding of the overall contributions of different inputs to the total  
240 uncertainty. The metals for which calculations were done were Al, Co, Ni, Cu, Zn, Cd and Pb,  
241 representing the set of metals for which field data were subsequently modelled. All calculations



242 represented the dissolved phase of surface waters. For Al a soft water composition broadly  
243 representative of the field samples simulated (Table 1) was used and calculations were done for the  
244 pH range 4.0 to 6.5. A FA concentration of  $10 \text{ mg L}^{-1}$  was used to simulate dissolved organic carbon.  
245 For the remaining metals, a harder water composition (Table 1) and a pH range of 5.0 to 8.5 was used.  
246 In both sets of calculations the dissolved Ca was adjusted to give charge balance at each pH value  
247 simulated.

248 Field datasets containing metal speciation data (free ion measurements) were compiled from the  
249 peer-reviewed literature. The datasets used are listed in Table 2 along with measurement methods. For  
250 all metals except Al, the datasets obtained were based on a complete review of the available literature.  
251 Data were used if the measurements of the free ion concentration, dissolved metal, DOC and pH were  
252 available. Measurements where prior adjustment of the pH to a quoted value was done were accepted,  
253 whereas measurements made on samples amended with additional metal were not. For Al, data were  
254 taken from three sites monitored under the UK Acid Waters Monitoring Scheme.<sup>[30]</sup> Al measurements  
255 in these samples did not comprise direct measurements of free ion concentration; instead,  $[\text{Al}^{3+}]$  was  
256 estimated by the speciation of measured 'labile' Al,<sup>[31]</sup> taken to comprise the free ion and all Al bound  
257 to inorganic ligands.

258 Concentrations of major dissolved species and other physicochemical parameters required for  
259 speciation calculations were obtained from the same literature source as the free metal ion  
260 concentrations, where possible. These included the temperature at the time of analysis, and  
261 concentrations of dissolved  $\text{Na}^+$ ,  $\text{Mg}^{2+}$ ,  $\text{Al}^{3+}$ ,  $\text{K}^+$ ,  $\text{Ca}^{2+}$ ,  $\text{Fe}^{3+}$ ,  $\text{Cl}^-$ ,  $\text{NO}_3^-$ ,  $\text{SO}_4^{2-}$  and F and alkalinity or  
262  $\text{CO}_3^{2-}$ . Where these measurements were not available, they were sourced from alternative literature, or  
263 were estimated (see Tables A1 and A2 in the Accessory publication). If measurements of carbonate or  
264 alkalinity were not available, equilibrium with atmospheric  $\text{CO}_2$  was assumed, using a partial pressure  
265 of 38.50 Pa (equivalent to  $3.80 \times 10^{-4}$  partial pressure). To check the sensitivity of the model to the  
266 chosen partial pressure we simulated the free metal ion concentrations in a freshwater medium at  
267 partial pressures between  $3.0 \times 10^{-4}$  and  $3.0 \times 10^{-3}$ . The calculated log free ion concentrations varied  
268 by no more 0.13.

269 In line with previous work,<sup>[19]</sup> the portion of DOC chemically active with respect to metal binding  
270 was represented by FA only and an 'activity factor',  $F_{\text{FADOC}}$ , was used to convert from measured DOC  
271 into model input FA. In this study we have used an  $F_{\text{FADOC}}$  value of 1.27, representing 63.5 % of the  
272 DOC being 'active' on average. This value was calculated from the geometric mean of  $F_{\text{FADOC}}$  values  
273 for a set of UK waters found by Bryan and coworkers (Fig. 1).<sup>[19]</sup> Where estimation of Al  
274 concentrations was not possible, dissolved Al was estimated by assuming that the solution was in  
275 equilibrium with aluminium(III) hydroxide. Dissolved iron(III) chemistry was simulated by allowing  
276 the precipitation of iron(III) hydroxide to occur and by allowing the precipitate to have a chemically

277 active surface. Iron(III) oxide was used as the model substance to simulate the surface chemistry of  
278 the precipitate, assuming one mole of precipitated iron(III) to form 90 g of oxide.<sup>[32]</sup>

279 Uncertainties considered in the speciation calculations are shown in Table 3. The uncertainty in log  
280  $K_{MA}$  for Model VII was set to the standard deviation of the fitted value<sup>[23]</sup> and for consistency the  
281 uncertainty in  $pK_{MH}$  values for metal binding to iron(III) oxide was set to the same value. The  
282 uncertainty in the solubility product of iron(III) hydroxide was derived from the calculations of the  
283 solubility product expression (see Accessory publication for details). For consistency the uncertainty  
284 in the solubility product of aluminium(III) hydroxide was set to the same value. For the theoretical  
285 calculations, separate model runs were done considering uncertainty in:

- 286 1.  $F_{FADOC}$  only;
- 287 2.  $F_{FADOC}$  and measurements;
- 288 3. parameters; and
- 289 4.  $F_{FADOC}$ , measurements and parameters.

290 For the calculations of free metal in the field datasets, the same runs were done except for ' $F_{FADOC}$   
291 only'. A sample size of 1999 was used to generate output distributions.

## 292 Results

### 293 *Modelling results: theoretical uncertainty calculations*

294 Calculations for Al are shown for pH 5.0 and pH 6.0 (Fig. 2). At pH 5.0, precipitation of  
295 aluminium(III) hydroxide was predicted not to occur in the majority of the Monte Carlo samples. By  
296 contrast, at pH 6.0, precipitation of aluminium(III) hydroxide was predicted to occur in all the Monte  
297 Carlo samples. Thus, at pH 6.0 calculated Al activities were controlled by the pH and the solubility of  
298 aluminium(III) hydroxide. Where only uncertainty in  $F_{FADOC}$  was considered, the calculated activity  
299 of  $Al^{3+}$  in equilibrium with the hydroxide was constant. Therefore, the only possible source of  
300 variability in calculated concentrations of  $[Al^{3+}]$  at pH 6.0 was variation in the calculated ionic  
301 strength, which was negligible. Hence the variability in calculated  $[Al^{3+}]$  (expressed as the  
302 interquartile range  $Q_{16-84}$ ) at pH 6.0 was also negligible when only uncertainty in  $F_{FADOC}$  was  
303 considered. At pH 5.0, in the absence of precipitation control, variability in  $[Al^{3+}]$  was controlled by  
304 the variability in input FA concentration imposed by the uncertainty in  $F_{FADOC}$ . Therefore, at this pH  
305 the variability as a result of uncertainty in  $F_{FADOC}$  was notably larger than at pH 6.0. This was also  
306 seen when uncertainties in measurements were considered along with the uncertainty in  $F_{FADOC}$ .  
307 Variability in  $[Al^{3+}]$  was similar at both pH 5.0 and pH 6.0 when uncertainty in parameters was  
308 considered, and in both cases was greater than the variability seen when uncertainties in  
309 measurements and  $F_{FADOC}$  were considered. At both pH values, the uncertainties in the log  $K_{MA}$  values  
310 for  $Al^{3+}$  and the competing ions  $Mg^{2+}$  and  $Ca^{2+}$  contributed to the variability. At pH 6.0, the  
311 uncertainty in the solubility product of Al hydroxide also contributed, resulting in a slightly larger

312 interquartile range. The variability obtained by combining different sources of uncertainty was clearly  
313 less than additive (on a log scale). Combining uncertainties attributable to  $F_{\text{FADOC}}$ , measurements and  
314 parameters produced similar variability at both pH values (1.28 at pH 5.0 and 1.20 at pH 6.0). The  
315 effect of combining uncertainties on the resulting variability was clearly less than additive. This was  
316 particularly clear at pH 5.0.

317 **Fig. 3** shows the variabilities in predicted free ion concentration for Co, Ni, Cu, Zn, Cd and Pb at  
318 pH 7.0. For Co and Ni, uncertainty in input measurements dominates the overall uncertainty, but  
319 uncertainty in  $F_{\text{FADOC}}$  does not contribute greatly to the measurement uncertainty. For Zn and Cd, the  
320 contributions of parameter uncertainty and of  $F_{\text{FADOC}}$  to measurement uncertainty are large relative to  
321 the other metals, particularly for Zn. The variability seen when considering measurements and  
322 parameters together is consistently less than additive. For Cu and Pb, uncertainties in parameters  
323 clearly make a larger contribution to the total variability than measurement uncertainties, and  
324 variability attributable to uncertainty in  $F_{\text{FADOC}}$  is approximately half that resulting from  
325 measurements overall. The relative importance of the different sources of uncertainty did not vary  
326 with pH (data not shown).

327 These calculations indicate that the sources of uncertainty in calculations are generally similar to  
328 those found by Groenenberg and coworkers<sup>[22]</sup> using the NICA–Donnan model. They found that  
329 uncertainties in binding predictions for Cu and Pb were largely attributable to uncertainty in the  
330 metals' binding affinity, which is consistent with our observation that parameter uncertainty  
331 (including uncertainty in the main metal binding parameter  $\log K_{\text{MA}}$ ) was more important than input  
332 measurement uncertainty for these metals. They also found that uncertainties in  $F_{\text{FADOC}}$  and in binding  
333 parameters produced comparable interquartile ranges of uncertainty for  $\text{Cd}^{2+}$ . This does not agree with  
334 our findings, where parameter uncertainty has a somewhat larger effect than uncertainty in  $F_{\text{FADOC}}$ .

### 335 *Modelling results: field data*

336 Model fits and the variability in outputs are given in **Tables 3** and **4**. The basic fit is characterised by  
337 the bias and the root mean squared error (RMSE) in  $\log [\text{M}^{z+}]$ .

338 Including a chemically active iron(III) oxide phase had a notable effect on the predicted speciation  
339 of lead. Free lead ion concentrations predicted, assuming precipitated iron(III) hydroxide to be surface  
340 active, were predicted to be up to almost two orders of magnitude lower than the concentrations  
341 predicted if precipitated iron(III) hydroxide was assumed to be not surface active (**Fig. 4**). This is in  
342 accordance with past modelling predictions<sup>[5]</sup> and with experimental observation (e.g. Lyvén et al.<sup>[33]</sup>)  
343 Negligible effects were seen for the other metals.

344 Observed and predicted concentrations of  $[\text{Al}^{3+}]$  (**Fig. 5**) had mean biases under 0.5 orders of  
345 magnitude for all three datasets. Dataset A1-01 had all observations predicted to within one order of  
346 magnitude and 52 of the 55 observations predicted to within 0.5 orders of magnitude. Dataset A1-02

347 had 179 of 180 observations predicted to within one order of magnitude and 162 observations  
348 predicted to within 0.5 orders of magnitude, and a small absolute bias (Table 5). Values in dataset AI-  
349 03 were not quite so well predicted with a relatively large negative bias. Of the observations, 141 of  
350 167 were predicted to within one order of magnitude. The number of observations predicted to within  
351 half an order of magnitude (59) was low relative to AI-01 and AI-02. Most observations fall within the  
352 interquartile range  $Q_{2.5-97.5}$ , suggesting that uncertainty in input variables and parameters can largely  
353 account for the discrepancies between observation and prediction.

354 Observed concentrations of  $[\text{Co}^{2+}]$  (Fig. 6) were all predicted to within one order of magnitude and  
355 six of the seven observations were predicted to within half an order of magnitude. One of the seven  
356 observations fell within the  $Q_{2.5-97.5}$  interquartile range.

357 Observed and predicted concentrations of  $[\text{Ni}^{2+}]$  (Fig. 7) showed that when  $[\text{Ni}^{2+}] > 10^{-8}$  M the  
358 model predictions were consistently within one order of magnitude of the observations with a mean  
359 bias of 0.06 log units. At lower concentrations, overestimation of observed  $[\text{Ni}^{2+}]$  was greater (mean  
360 bias 0.82 log units). This tendency to overestimation has been noted previously<sup>[34,35]</sup> when using  
361 Model VI. Overall, 43 of 54 observations were predicted to within one order of magnitude, and 21 to  
362 within 0.5 orders of magnitude.

363 Observed and predicted concentrations of  $[\text{Cu}^{2+}]$  (Fig. 8) showed that agreement between  
364 observation and prediction was better at higher free copper ( $>10^{-12}$  M) than at lower concentrations.  
365 Overall 33 of 133 observations were predicted to within one order of magnitude and 21 to within 0.5  
366 orders of magnitude. The data for which  $[\text{Cu}^{2+}] < 10^{-12}$  M have all been measured using voltammetric  
367 techniques. Measured  $[\text{Cu}^{2+}]$  ranges were as low as  $10^{-16}$  M yet the model did not predict any  
368 concentrations to be below  $10^{-13}$  M. Mean biases for four of the five datasets obtained using  
369 competitive ligand exchange–adsorptive cathodic stripping voltammetry (CLE-AdCSV) (Cu-02 to  
370 Cu-05) showed overestimation of measured concentrations by at least two orders of magnitude on  
371 average. By contrast, the concentrations in dataset Cu-01, also measured by CLE-AdCSV, were  
372 underestimated by the model. Seven of nine CLE-AdCSV measurements in dataset Cu-03 with  
373 observed  $[\text{Cu}^{2+}]$  in the range  $10^{-12}$  to  $10^{-9}$  M, were relatively well predicted, to within an order of  
374 magnitude. These measurements were done in soft, acidic-to-circumneutral waters (pH 5.3–7.5;  
375 dissolved Ca 42–85 mg L<sup>-1</sup>) of low [DOC] (0.4–1.1 mg C L<sup>-1</sup>) whereas the remaining measurements  
376 were done in waters of higher pH (samples were adjusted to pH 7.9), hardness (dissolved Ca 0.1–0.4  
377 mg L<sup>-1</sup>) and [DOC] (0.9–5.8 mg C L<sup>-1</sup>).

378 The other measurement techniques used generally resulted in closer agreement between  
379 observation and prediction. For measurements using the DMT (Cu-06b, Cu-07 and Cu-08), bias  
380 between observation and prediction was fairly low, but there was notable scatter between observation  
381 and prediction when  $[\text{Cu}^{2+}] < 10^{-9}$  M. Dataset Cu-06a (permeation liquid membrane) was

382 underestimated on average. Dataset Cu-09, obtained using an ion exchange column method (IET),  
383 showed relatively close agreement between observation and prediction when  $[Cu^{2+}] > 10^{-8}$  M (mean  
384 bias =  $-0.12$  log units). At lower free copper concentrations agreement was relatively poor (mean bias  
385 =  $-2.22$  log units).

386 Observed and predicted concentrations of  $[Zn^{2+}]$  (Fig. 9) showed that 72 of 84 observations were  
387 predicted to within an order of magnitude and 45 to within half an order of magnitude. Some patterns  
388 can be observed depending upon measurement technique. Observations obtained by CLE-AdCSV  
389 (Zn-01, Zn-02, Zn-03) were mostly overestimated by the model (mean bias 0.5 log units).  
390 Observations obtained by DMT (Zn-04, Zn-05) were correlated fairly well with prediction when  
391  $[Zn^{2+}] > 10^{-7}$  M (RMSE 0.12 log units) although with a relatively small bias to underestimation (mean  
392  $-0.26$  log units). For  $[Zn^{2+}] < 10^{-7}$  M, observations obtained by DMT became more scattered with  
393 respect to predictions (RMSE 0.26 log units). Observations obtained by IET (Zn-06) were predicted  
394 relatively well when  $[Zn^{2+}] > 10^{-7}$  M (mean bias  $-0.14$  log units) but were not so well predicted at  
395 lower concentrations (mean bias  $-0.91$  log units).

396 Observed and predicted concentrations of  $[Cd^{2+}]$  (Fig. 10) showed patterns generally similar to  
397 those for zinc. Of 85 measurements, 72 were predicted to within an order of magnitude and 51 to  
398 within half an order of magnitude. Measurements made using voltammetric techniques (Cd-01, Cd-  
399 02) were consistently overpredicted. Measurements made using DMT were simulated relatively well  
400 (RMSE 0.06 log units, mean bias 0.08 log units) when  $[Cd^{2+}] > 10^{-10}$  M but were overpredicted at  
401 lower concentrations (mean bias 0.68 log units). Observations made using IET were all simulated to  
402 within one order of magnitude. Two of three measurements made using a permeation liquid  
403 membrane (PLM) were predicted to within one order of magnitude.

404 Table 5 compares bias and error in the predictions made with and without assuming binding of lead  
405 to iron(III) oxide. Allowing precipitated iron(III) hydroxide to have an active surface either reduced  
406 the predicted free ion or made little difference to the prediction. Overall, bias and RMSE were  
407 reduced by allowing precipitated iron(III) hydroxide to have an active surface. Of the individual  
408 datasets, the fit was most improved for Pb-01, for which the binding to iron(III) oxide is most  
409 important in determining the predicted free ion (Fig. 4) although the bias and RMSE remained large.

410 Observed and predicted concentrations of  $[Pb^{2+}]$ , assuming binding of lead to iron(III) oxide (Fig.  
411 11), showed somewhat similar patterns to Cu. Measurements made using competitive ligand  
412 exchange–differential pulse cathodic stripping voltammetry (CLE-DPCSV) were consistently  
413 underpredicted. Measurements made by DMT were predicted with low bias but with notable scatter  
414 (21 of 45 observations were not predicted to within one order of magnitude). Two of three  
415 measurements made by PLM were predicted to within an order of magnitude. Overall, 33 of 76

416 observations were predicted to within one order of magnitude and 19 to within 0.5 orders of  
417 magnitude.

#### 418 *Model uncertainty*

419 Model uncertainty results (Tables 4, 5) summarise the spread of output values (quantified as the  $Q_{16-84}$   
420 interquartile range of log free ion concentration) obtained in each dataset when considering  
421 uncertainty in (a) input variables and  $F_{\text{FADOC}}$  only, (b) parameters only, and (c) input variables,  $F_{\text{FADOC}}$   
422 and parameters together. The influence of the different categories of uncertainty on the variability of  
423 the output free ion concentrations is not additive, consistent with the findings of the theoretical  
424 calculations. Where uncertainties in inputs,  $F_{\text{FADOC}}$  and parameters are considered together, the spread  
425 of output values is smaller than the sum of the corresponding ranges calculated when the uncertainties  
426 are considered in separate simulations. With the exception of Cu, considering input uncertainty only  
427 mostly results in a greater spread of output predictions than does considering parameter uncertainty  
428 only. Parameter uncertainty resulted in a greater spread of output predictions in one of three Al  
429 datasets, and in two of five Pb datasets. For Cu, considering parameter uncertainty resulted in spreads  
430 of output values that were consistently greater than or equal to the spreads obtained when  
431 uncertainties in inputs and  $F_{\text{FADOC}}$  were considered. On average, the spreads of output values (i.e. the  
432 breadth of the  $Q_{16-84}$  range) followed the trend  $\text{Al} \approx \text{Cu} > \text{Pb} > \text{Ni} \approx \text{Zn} \approx \text{Cd}$ .

433 A key aspect of assessing uncertainty is whether discrepancies between observations and  
434 predictions can generally be attributed to uncertainty in the input variables and model parameters, i.e.  
435 if the observation falls within the range of predicted values then the discrepancy is explained. The  
436  $Q_{2.5-97.5}$  interquartile range of the predictions, when all uncertainties were considered, was used to  
437 assess this (Tables 3, 4).

438 The majority of observations of  $[\text{Al}^{3+}]$  (88 %) fell within the  $Q_{2.5-97.5}$  range and so generally the  
439 discrepancies can be attributed to the influence of uncertainties. However, for the other metals, the  
440 proportions of observations falling within this range were lower, ranging from 0 % for Co to 42 % for  
441 Cd, and 22 % when all five metals were considered together. Thus, in general the discrepancies  
442 between observation and prediction could not be attributed to uncertainty in the model predictions.

#### 443 **Discussion**

444 As noted in the Introduction, the following factors must be considered when the performance of  
445 WHAM/Model VII is assessed against field observations:

- 446 • the influences of uncertainties in model inputs variables and parameters on the spread of model  
447 predictions;
- 448 • the extent to which the metal binding properties of humic substances represent those of field  
449 DOM; and

450 • the accuracy and precision of measured free metal ion concentrations.

451 This study has explicitly tackled the first of these factors, by incorporating the consideration of  
452 uncertainty in input variables and parameters into the model to allow a spread of predictions that can  
453 be compared to measured values. The second factor was partly tackled by incorporating uncertainty in  
454  $F_{\text{FADOC}}$  into calculations. We have shown that with the exception of Al, discrepancies between  
455 measurements and model predictions can largely not be explained by uncertainties in input variables  
456 or model parameters, assuming that such uncertainties have been reasonably quantified. Two factors  
457 thus remain as possible sources of discrepancy between model and measurement: the extent to which  
458 isolated humic substances represent field DOM, and the precision and accuracy of free ion  
459 measurements.

460 In this study we have simulated metal speciation assuming DOM to comprise a mixture of FA and  
461 an undefined, ‘inert’ material having no ion-binding properties. No other organic ligands are  
462 considered. Non-humic, metal-binding organic ligands could influence speciation if present in  
463 sufficient quantities to compete with FAs. This is not, however, a structural issue with the model, but  
464 a limitation of the ability to characterise and model all the significant individual components of DOM.  
465 Some researchers have suggested a significant role for non-humic ligands in controlling freshwater  
466 metal speciation. For example, Xue and Sigg<sup>[36]</sup> suggested that the strong binding and low free ion  
467 concentrations of copper and cadmium found in some Swiss lakes were attributable to small amounts  
468 of ligands having stronger binding than humic substances, Rozan and Benoit<sup>[37]</sup> suggested that copper  
469 speciation in rivers of southern New England was controlled in part by sulphide and  
470 ethylenediaminetetraacetic acid (EDTA), and Baken et al.<sup>[38]</sup> found that EDTA was an important  
471 control on metal speciation in anthropogenically affected waters, particularly for Ni. Thus, where the  
472 model overestimates the observed free ion it is reasonable to postulate that this may be attributable to  
473 unaccounted-for strong ligands. Clearly there is a need to further investigate the occurrence and  
474 metal-binding properties of such ligands. Methods to distinguish different types of DOM in waters  
475 exist (e.g. Murphy et al.<sup>[39]</sup>) and research on structural identification of individual DOM components  
476 (e.g. Woods et al.<sup>[40]</sup>) is ongoing. Parallel application of such methods in speciation studies may assist  
477 in identifying and characterising non-humic components of DOM and their role in metal binding.

478 We now turn to the precision and accuracy of measurements of the free metal ion. Of the two,  
479 precision (i.e. reproducibility) is the easier to quantify. We did not consider precision when analysing  
480 the agreement between model and prediction, because it was not quantified in all the studies and so a  
481 consistent analysis of its role was not feasible. More emphasis is needed on quantifying the precision  
482 of speciation measurements, as it is a key aspect of the assessment both of the method and of the  
483 comparative performance of speciation models. Measurement accuracy is more challenging to assess,  
484 particularly for the complex methods used to measure free metal ions. Method validation in simple  
485 matrices under laboratory conditions may not hold in the more complex chemical environment

486 presented by a field sample. The accuracy of speciation methods has accordingly been questioned in  
487 the literature. For example, van Leeuwen and Town<sup>[41]</sup> have questioned the results of competitive  
488 ligand exchange voltammetry, arguing that equilibrium between the natural and added competing  
489 ligands is not necessarily attained within the experimental timeframe, and that this introduces bias into  
490 the reported free ion concentrations by underestimation of the actual equilibrium value. In this case,  
491 the argument against the accuracy of the method is consistent with the model predictions in that  
492 WHAM tends to predict a higher free metal ion than is measured by voltammetry. Comparing the  
493 model with those datasets not obtained using voltammetry produces decreases in bias for Cu, Cd and  
494 Pb, and RMSE for Cu, Zn, Cd and Pb (Table 6). However, this cannot be taken as definitive evidence  
495 that voltammetry gives inaccurate measurements, as this would mean assuming that the model  
496 predictions are accurate. More systematic evaluation of the accuracy of speciation methods is needed.  
497 A useful first step would be to move towards standardisation of methods, to make their  
498 intercomparison more reliable.<sup>[42]</sup> Intercomparison among methods should provide insights not  
499 obtainable by comparison solely with models that are based on key a-priori assumptions about the  
500 system under study. This is not to say, however, that models do not have a useful role to play in the  
501 evaluation of measurement methods. Models provide an internally consistent set of predictions against  
502 which to compare multiple measurement methods and gain additional information on the relative  
503 performance of different methods under different chemical conditions. The collation of literature data  
504 presented here shows that comparative measurements are rare, being confined to one study. Unsworth  
505 and coworkers<sup>[16]</sup> compared DMT and PLM measurements of free ionic Cu and Pb in three samples  
506 and of Cd in two samples. This study is a beginning, but as the number of samples is limited there is  
507 currently little scope to systematically assess the relative performance of the methods.

508 If the observations obtained using voltammetry are excluded, the bias between the model  
509 predictions and observations is below 0.5 orders of magnitude for all the metals except Ni (Tables 5,  
510 6). Bias above 0.5 orders of magnitude in individual datasets, e.g. Al-03 and Cd-04, could be reduced  
511 by model ‘calibration’, such as adjustment of  $F_{\text{FADOC}}$  within plausible ranges. A recent modelling  
512 study of Al speciation data from the UK Acid Waters Monitoring Network<sup>[43]</sup> showed that the data  
513 could be simulated using plausible general values of  $F_{\text{FADOC}}$ , one for streams and one for lakes, similar  
514 in magnitude to the central value adopted here.

515 Speciation models are increasingly being incorporated into risk assessment models such as the  
516 Biotic Ligand Model (BLM).<sup>[44]</sup> Accuracy and precision of speciation model predictions are thus  
517 important for the accuracy and precision of the predictions of such models. Judgements as to what  
518 constitutes ‘reasonable’ or ‘acceptable’ accuracy and precision in model predictions are contingent on  
519 the purpose of the specific model. For example, the purpose of the BLM is to describe the variability  
520 in metal toxicity across varying water compositions. The BLM has been shown to accomplish this  
521 purpose for several metals and organisms (e.g. De Schamphelaere and Janssen<sup>[45]</sup> and De



522 Schampelaere et al.<sup>[46]</sup>). This suggests that the humic-binding submodel in the BLM is performing  
523 well under the conditions of the metal toxicity tests, although bias in the model predictions will be  
524 compensated for to some extent if the BLM is calibrated using data generated in waters containing  
525 DOM. The performance of the BLM is qualitatively consistent with the observation, in the current  
526 study, that WHAM predictions of the free metal ion tend to agree with observations best when the  
527 latter are relatively high, where toxic effects are most likely to be seen under laboratory conditions  
528 ( $\sim 10^{-8}$  M,  $10^{-9}$  M,  $10^{-7}$  M,  $10^{-10}$  M and  $10^{-9}$  M for Ni, Cu, Zn, Cd and Pb). It is feasible that future  
529 extension of the BLM to chronic effects of sensitive freshwater organisms may extend the range of its  
530 application to lower free ion concentrations, where agreement between observation and model  
531 prediction is sometimes poorer. This possibility needs to be borne in mind in future development of  
532 biotic ligand models. Ideally, the influence of uncertainty in WHAM predictions should be  
533 incorporated into biotic ligand models so that the propagation of uncertainties into predictions of  
534 toxicity can be assessed. Similar considerations apply to other environmental models having a  
535 speciation component, such as CHUM<sup>[47]</sup> and TICKET-UWM.<sup>[48]</sup>

536 A full consideration of the performance of WHAM, or any other model, can only ideally be done if  
537 the precision of the observations and variability in the model predictions can be quantified and the  
538 accuracy of the observations can be relied upon. In this study we have made a first quantification of  
539 the uncertainty (i.e. the variability) of the model predictions and a comparison of predictions with  
540 available observations. A possible next step would be to extend the calculation of uncertainty to  
541 include solution complexation. This has been previously done for actinides,<sup>[49]</sup> where complexation to  
542 inorganic ligands such as carbonate may be important. Looking to the future, we would recommend  
543 the following research steps to progress the understanding and assessment of metal speciation  
544 measurement and modelling in freshwaters:

- 545 • A more comprehensive approach to speciation measurements, including the simultaneous testing  
546 of multiple methods and parallel characterisation of DOM structure and composition, in as wide a  
547 range of waters as possible.
- 548 • Explicit and routine consideration of the influence of model uncertainty on the outputs of  
549 geochemical and toxicity models, and assessment of the implications for specific model  
550 applications such as risk assessment.

## 551 **Conclusions**

- 552 • Discrepancies between observations and predictions of free Al were generally attributable to  
553 uncertainties in input variables and model parameters, however, this was not the case for Co, Ni,  
554 Cu, Zn, Cd and Pb.
- 555 • Generally, the best agreements between measurements and predictions were seen for Al, Co, Ni,  
556 Zn and Cd. Agreements for Cu and Pb were dependent upon the analytical method used to

557 measure the free ion: measurements made using voltammetry were largely overestimated by the  
558 model. Generally, the model agreed best with measurements made using the DMT, IET and PLM  
559 methods.

560 • More parallel comparisons of multiple analytical methods and modelling are needed to better  
561 understand the reasons for the observed patterns and discrepancies between observations and  
562 model predictions. More comprehensive characterisation of the different components of DOM is  
563 needed.

564 • More emphasis needs to be placed generally on quantifying the precision (uncertainty) of  
565 measurements and model predictions, as this is essential for assessing the accuracy of model  
566 predictions.

### 567 **Glossary of terms and parameters used in this study**

568  $n_A$ , density of Type A binding sites on humic or fulvic acid

569  $K_{A/B}$ , equilibrium constant for proton binding to Type A or Type B sites on humic or fulvic acid (Eqn 1)

570  $K_{MA/MB}$ , equilibrium constant for metal binding to Type A or Type B sites on humic or fulvic acid (Eqn 2)

571  $\Delta LK_2$ , heterogeneity term used to generate strong metal binding sites on humic or fulvic acid

572  $K_{1,oxide}$ , equilibrium constant for protonation of metal oxide surface site (Eqn 5)

573  $K_{2,oxide}$ , equilibrium constant for deprotonation of metal oxide surface site (Eqn 6)

574  $K_{MH,oxide}$ , equilibrium constant for metal-proton exchange at metal oxide surface site (Eqn 7)

575  $\Delta pK_{MH,oxide}$ , heterogeneity term used to generate strong metal binding sites on metal oxide surface

576  $x_i$ , central value of input variable or parameter for which uncertainty is to be considered

577  $x'_{i,j}$ , perturbed value of input variable or parameter, used for calculation of speciation in a single Monte Carlo  
578 sample

579  $q$ , perturbation factor used to generate  $x'_{i,j}$  values, generated by random sampling from a standard normal  
580 distribution

581  $\sigma_i$ , uncertainty factor for input variable or parameter having absolute uncertainty

582  $p_i$ , uncertainty factor for input variable or parameter having relative uncertainty

583  $F_{FADOC}$ , factor relating observed dissolved organic carbon concentrations to fulvic acid concentrations for the  
584 purposes of speciation calculation. A value of two indicates that DOC is 100% active with respect to ion  
585 binding

586  $Q_{16-84}$ , the interquartile range between the 16th and 84th percentiles of the distribution of calculated free metal  
587 ion concentrations

588  $Q_{2.5-97.5}$ , the interquartile range between the 2.5th and 97.5th percentiles of the distribution of calculated free  
589 metal ion concentrations

590 bias, the mean of absolute deviations between observed and calculated log [free ion] in a dataset. A positive bias  
591 indicates that on average predicted concentrations exceed observed ones, and vice versa.

## 592 **Accessory publication**

593 Additional information on the sources of pH, DOC and major solute concentrations used in the field  
594 study modelling, and the calculation of the solubility express ion for iron(III) hydroxide, is given in  
595 the Accessory publication (see [http://www.publish.csiro.au/?act =](http://www.publish.csiro.au/?act=view_file&file_id=EN11049_AC.pdf)  
596 [view\\_file&file\\_id=EN11049\\_AC.pdf](http://www.publish.csiro.au/?act=view_file&file_id=EN11049_AC.pdf)).

## 597 **Acknowledgements**

598 The authors thank K. Delbeke, C. E. Schlekot, I. Schoeters, J. Meyer, R. L. Dwyer, D. S. Smith and R. C.  
599 Santore for their comments and suggestions on the report from which this paper was developed. They also thank  
600 Don Monteith for providing aluminium speciation data from the UK Acid Waters Monitoring Network, and  
601 Claude Fortin and Peter Campbell for providing the raw data for datasets Cu-09, Zn-06 and Cd-06. This work  
602 was funded by the following organisations: International Copper Association (ICA), International Council on  
603 Mining and Minerals (ICMM), International Lead Zinc Research Organization (ILZRO), Nickel Producers  
604 Environmental Research Association (NiPERA), Cobalt Development Institute (CDI), Rio Tinto Minerals,  
605 International Chromium Development Association (ICDA), International Molybdenum Association (IMOA),  
606 European Aluminium Association (EAA), UK Natural Environment Research Council (NERC).

## 607 **References**

608

- 609 [1] M. F. Benedetti, C. J. Milne, D. G. Kinniburgh, W. H. van Riemsdijk, L. K. Koopal, Metal ion binding to  
610 humic substances: application of the nonideal competitive adsorption model. *Environ. Sci. Technol.* 1995, 29,  
611 446.
- 612 [2] E. Tipping, Humic Ion Binding Model VI: an improved description of the interactions of protons and metal  
613 ions with humic substances. *Aquat. Geochem.* 1998, 4, 3.
- 614 [3] E. Tipping, WHAM – a chemical-equilibrium model and computer code for waters, sediments, and soils  
615 incorporating a discrete site electrostatic model of ion-binding by humic substances. *Comput. Geosci.* 1994, 20,  
616 973.
- 617 [4] D. N. Di Toro, H. E. Allen, H. L. Bergman, J. S. Meyer, P. R. Paquin, R. C. Santore, Biotic ligand model of  
618 the acute toxicity of metals. 1. Technical basis. *Environ. Toxicol. Chem.* 2001, 20, 2383.
- 619 [5] S. Lofts, E. Tipping, Solid-solution metal partitioning in the Humber Rivers: application of WHAM and  
620 SCAMP. *Sci. Total Environ.* 2000, 251–252, 381.
- 621 [6] E. J. J. Kalis, L. Weng, F. Dousma, E. J. M. Temminghoff, W. H. van Riemsdijk, Measuring free metal ion  
622 concentrations in situ in natural waters using the Donnan membrane technique. *Environ. Sci. Technol.* 2006, 40,  
623 955.

- 624 [7] J. Qian, H. B. Xue, L. Sigg, A. Albrecht, Complexation of cobalt by natural ligands in freshwater. *Environ.*  
625 *Sci. Technol.* 1998, 32, 2043.
- 626 [8] S. Meylan, N. Odzak, R. Behra, L. Sigg, Speciation of copper and zinc in natural freshwater: comparison of  
627 voltammetric measurements, diffusive gradients in thin films (DGT) and chemical equilibrium models. *Anal.*  
628 *Chim. Acta* 2004, 510, 91.
- 629 [9] H. B. Xue, A. Oestreich, D. Kistler, L. Sigg, L., Free cupric ion concentrations and Cu complexation in  
630 selected Swiss lakes and rivers. *Aquat. Sci.* 1996, 58, 69.
- 631 [10] A. Plöger, E. Fischer, H.-P. Nirmaier, L. M. Laglera, D. Monticelli, C. M. G. van den Berg, Lead and  
632 copper speciation in remote mountain lakes. *Limnol. Oceanogr.* 2005, 50, 995.
- 633 [11] H. B. Xue, L. Sigg, Free cupric ion concentration and CuII speciation in a eutrophic lake. *Limnol.*  
634 *Oceanogr.* 1993, 38, 1200.
- 635 [12] H. B. Xue, L. Sigg, Zinc speciation in lake waters and its determination by ligand-exchange with EDTA  
636 and differential-pulse anodic-stripping voltammetry. *Anal. Chim. Acta* 1994, 284, 505.
- 637 [13] J. Cao, H. B. Xue, L. Sigg, Effects of pH and Ca competition on complexation of cadmium by fulvic acids  
638 and by natural organic ligands from a river and a lake. *Aquat. Geochem.* 2006, 12, 375.
- 639 [14] C. Fortin, P. G. C. Campbell, An ion-exchange technique for free-metal ion measurements (Cd<sup>2+</sup>, Zn<sup>2+</sup>):  
640 applications to complex aqueous media. *Int. J. Environ. Anal. Chem.* 1998, 72, 173.
- 641 [15] Y. Gopalapillai, C. L. Chakrabarti, D. R. S. Lean, Assessing toxicity of mining effluents: equilibrium- and  
642 kinetics-based metal speciation and algal bioassay. *Environ. Chem.* 2008, 5, 307.
- 643 [16] E. R. Unsworth, K. W. Warnken, H. Zhang, W. Davison, F. Black, J. Buffle, J. Cao, R. Cleven, J.  
644 Galceran, P. Gunkel, E. Kalis, D. Kistler, H. P. van Leeuwen, M. Martin, S. Noël, Y. Nur, N. Odzak, J. Puy, W.  
645 van Riemsdijk, L. Sigg, E. J. M. Temminghoff, M.-L. Tercier-Waeber, S. Topperwien, R. M. Town, L. Weng,  
646 H. B. Xue, Model predictions of metal speciation in freshwaters compared to measurements by in situ  
647 techniques. *Environ. Sci. Technol.* 2006, 40, 1942.
- 648 [17] Y. Gopalapillai, I. I. Fafous, J. D. Murimboh, T. Yapici, P. Chakraborty, C. L. Chakrabarti, Determination  
649 of free nickel ion concentrations using the ion exchange technique: application to aqueous mining and municipal  
650 effluents. *Aquat. Geochem.* 2008, 14, 99.
- 651 [18] E. J. M. Temminghoff, A. C. C. Plette, R. van Eck, W. H. Van Riemsdijk, Determination of the chemical  
652 speciation of trace metals in aqueous systems by the Wageningen Donnan Membrane technique. *Anal. Chim.*  
653 *Acta* 2000, 417, 149.
- 654 [19] S. E. Bryan, E. Tipping, J. Hamilton-Taylor, Comparison of measured and modelled copper binding by  
655 natural organic matter in freshwater. *Comp. Biochem. Physiol. C* 2002, 133, 37.
- 656 [20] E. Tipping, C. Woof, M. A. Hurley, Humic substances in acid surface waters; modelling aluminium  
657 binding, contribution to ionic charge-balance, and control of pH. *Water Res.* 1991, 25, 425.

- 658 [21] G. M. Anderson, Error propagation by the Monte Carlo method in geochemical calculations. *Geochim.*  
659 *Cosmochim. Acta* 1976, 40, 1533.
- 660 [22] J. E. Groenenberg, G. F. Koopmans, R. N. J. Comans, Uncertainty analysis of the nonideal competitive  
661 adsorption–Donnan model: effects of dissolved organic matter variability on predicted metal speciation in soil  
662 solution. *Environ. Sci. Technol.* 2010, 44, 1340.
- 663 [23] E. Tipping, S. Lofts, J. E. Sonke, Humic Ion-Binding Model VII: a revised parameterisation of cation-  
664 binding by humic substances. *Environ. Chem.* 2011, 8, 225.
- 665 [24] S. Lofts, E. Tipping, An assemblage model for cation binding by natural particulate matter. *Geochim.*  
666 *Cosmochim. Acta* 1998, 62, 2609.
- 667 [25] E. Tipping, C. Rey-Castro, S. E. Bryan, J. Hamilton-Taylor, AlIII and FeIII binding by humic substances  
668 in freshwaters, and implications for trace metal speciation. *Geochim. Cosmochim. Acta* 2002, 66, 3211.
- 669 [26] S. Lofts, E. Tipping, J. Hamilton-Taylor, The chemical speciation of FeIII in freshwaters. *Aquat.*  
670 *Geochem.* 2008, 14, 337.
- 671 [27] X. Liu, F. J. Millero, The solubility of iron hydroxide in sodium chloride solutions. *Geochim. Cosmochim.*  
672 *Acta* 1999, 63, 3487.
- 673 [28] D. T. Monteith, C. D. Evans, The United Kingdom Acid Waters Monitoring Network: a review of the first  
674 15 years and introduction to the special issue. *Environ. Pollut.* 2005, 137, 3.
- 675 [29] C. T. Driscoll, A procedure for the fractionation of aqueous aluminium in dilute acid waters. *Int. J.*  
676 *Environ. Anal. Chem.* 1984, 16, 267.
- 677 [30] D. A. Dzombak, F. M. M. Morel, *Surface Complexation Modeling: Hydrous Ferric Oxide* 1990 (Wiley:  
678 New York).
- 679 [31] B. Lyvén, M. Hasselov, D. R. Turner, C. Haraldsson, K. Andersson, Competition between iron- and  
680 carbon-based colloidal carriers for trace metals in a freshwater assessed using flow field-flow fractionation  
681 coupled to ICPMS. *Geochim. Cosmochim. Acta* 2003, 67, 3791.
- 682 [32] J. A. B. Bass, R. Blust, R. T. Clarke, T. A. Corbin, W. Davison, K. A. C. De Schamphelaere, C. R.  
683 Janssen, E. J. J. Kalis, M. G. Kelly, N. T. Kneebone, A. J. Lawlor, S. Lofts, E. J. M. Temminghoff, S. A.  
684 Thacker, E. Tipping, C. D. Vincent, K. W. Warnken, H. Zhang, *Environmental Quality Standards for trace*  
685 *metals in the aquatic environment. Environment Agency Science Report – SC030194* 2008 (Environment  
686 Agency: Bristol, UK).
- 687 [33] L. Van Laer, E. Smolders, F. Degryse, C. Janssen, K. A. C. De Schamphelaere, Speciation of nickel in  
688 surface waters measured with the Donnan membrane technique. *Anal. Chim. Acta* 2006, 578, 195.
- 689 [34] H. B. Xue, L. Sigg, Comparison of the complexation of Cu and Cd by humic or fulvic acids and by ligands  
690 observed in lake waters. *Aquat. Geochem.* 1999, 5, 313.
- 691 [35] T. F. Rozan, G. Benoit, Geochemical factors controlling free Cu ion concentrations in river water.  
692 *Geochim. Cosmochim. Acta* 1999, 63, 3311.

- 693 [36] S. Baken, F. Degryse, L. Verheyen, R. Merckx, E. Smolders, Metal complexation properties of freshwater  
694 dissolved organic matter are explained by its aromaticity and by anthropogenic ligands. *Environ. Sci. Technol.*  
695 2011, 45, 2584.
- 696 [37] K. R. Murphy, C. A. Stedmon, T. D. Waite, G. M. Ruiz, Distinguishing between terrestrial and  
697 autochthonous organic matter sources in marine environments using fluorescence spectroscopy. *Mar. Chem.*  
698 2008, 108, 40.
- 699 [38] G. C. Woods, M. J. Simpson, P. J. Koerner, A. Napoli, A. J. Simpson, HILIC-NMR: toward the  
700 identification of individual molecular components in dissolved organic matter. *Environ. Sci. Technol.* 2011, 45,  
701 3880.
- 702 [39] H. P. van Leeuwen, R. M. Town, Kinetic limitations in measuring stabilities of metal complexes by  
703 competitive ligand exchange-adsorptive stripping voltammetry (CLEAdSV). *Environ. Sci. Technol.* 2005, 39,  
704 7217.
- 705 [40] M. Filella, R. Town, J. Buffle, Speciation in freshwaters, in *Chemical speciation in the environment* (Eds.  
706 A. M. Ure, C. M. Davidson) 1995, pp. 169–200 (Chapman & Hall: Glasgow).
- 707 [41] E. Tipping, H. T. Carter, Aluminium speciation in streams and lakes of the UK Acid Waters Monitoring  
708 Network, modelled with WHAM. *Sci. Total Environ.* 2011, 409, 1550.
- 709 [42] D. M. Di Toro, H. E. Allen, H. L. Bergman, J. S. Meyer, P. R. Paquin, R. C. Santore, Biotic ligand model  
710 of the acute toxicity of metals. 1. Technical basis. *Environ. Toxicol. Chem.* 2001, 20, 2383.
- 711 [43] K. A. C. De Schamphelaere, C. R. Janssen, Development and field validation of a biotic ligand model  
712 predicting chronic copper toxicity to *Daphnia magna*. *Environ. Toxicol. Chem.* 2004, 23, 1365.
- 713 [44] K. A. C. De Schamphelaere, S. Lofts, C. R. Janssen, Bioavailability models for predicting acute and  
714 chronic toxicity of zinc to algae, daphnids, and fish in natural surface waters. *Environ. Toxicol. Chem.* 2005, 24,  
715 1190.
- 716 [45] E. Tipping, A. J. Lawlor, S. Lofts, L. Shotbolt, Simulating the long-term chemistry of an upland UK  
717 catchment: heavy metals. *Environ. Pollut.* 2006, 141, 139.
- 718 [46] K. J. Farley, R. F. Carbonaro, C. J. Fanelli, R. Costanzo, K. J. Rader, D. M. Di Toro, TICKET-UWM: a  
719 coupled kinetic, equilibrium, and transport screening model for metals in lakes. *Environ. Toxicol. Chem.* 2011,  
720 30, 1278.
- 721 [47] F. H. Denison, J. Garnier-Laplace, The effects of database parameter uncertainty on uranium(VI)  
722 equilibrium calculations. *Geochim. Cosmochim. Acta* 2005, 69, 2183.
- 723 [48] J. W. Guthrie, N. M. Hassan, M. S. A. Salam, I. I. Fafous, C. A. Murimboh, J. Murimboh, C. L.  
724 Chakrabarti, D. C. Grégoire, Complexation of Ni, Cu, Zn, and Cd by DOC in some metal-impacted freshwater  
725 lakes: a comparison of approaches using electrochemical determination of free-metal-ion and labile complexes  
726 and a computer speciation model, WHAM V and VI. *Anal. Chim. Acta* 2005, 528, 205.

727 [49] C. Fortin, Y. Couillard, B. Vigneault, P. G. C. Campbell, Determination of Free Cd, Cu and Zn  
728 concentrations in lake waters by in situ diffusion followed by column equilibration ion-exchange. *Aquat.*  
729 *Geochem.* 2010, 16, 151.

730 Manuscript received 13 April 2011, accepted 26 July 2011

731

732

**Table 1. Water compositions used for theoretical calculations**

733

M = Co, Ni, Cu, Zn, Cd, Pb; FA = fulvic acid

Determinand	Composition for calculation of uncertainty in [Al <sup>3+</sup> ]	Composition for calculation of uncertainty in [M <sup>2+</sup> ]
Temperature (K)	293	293
FA (mg L <sup>-1</sup> )	10.0	5.0
Dissolved Na (M)	$1.0 \times 10^{-4}$	$5.0 \times 10^{-4}$
Dissolved Mg (M)	$5.0 \times 10^{-5}$	$5.0 \times 10^{-4}$
Dissolved Al (M)	$5.0 \times 10^{-6}$ <sup>A</sup>	$1.0 \times 10^{-5}$ <sup>A</sup>
Dissolved K (M)	$1.0 \times 10^{-5}$	$5.0 \times 10^{-5}$
Dissolved Ca (M) <sup>B</sup>	$5.1 \times 10^{-5}$ – $1.3 \times 10^{-4}$	$4.7 \times 10^{-4}$ – $1.7 \times 10^{-3}$
Dissolved Fe <sup>III</sup> (M)	$1.0 \times 10^{-6}$ <sup>A</sup>	$1.0 \times 10^{-6}$ <sup>A</sup>
Dissolved Co (M)	–	$1.0 \times 10^{-9}$
Dissolved Ni (M)	–	$5.0 \times 10^{-9}$
Dissolved Cu (M)	–	$2.0 \times 10^{-8}$
Dissolved Zn (M)	–	$1.0 \times 10^{-7}$
Dissolved Cd (M)	–	$1.0 \times 10^{-9}$
Dissolved Pb (M)	–	$1.0 \times 10^{-8}$
Dissolved Cl (M)	$5.0 \times 10^{-4}$	$1.0 \times 10^{-3}$
Dissolved NO <sub>3</sub> (M)	$5.0 \times 10^{-6}$	$5.0 \times 10^{-4}$
Dissolved SO <sub>4</sub> (M)	$1.0 \times 10^{-4}$	$5.0 \times 10^{-4}$
pCO <sub>2</sub> (Pa)	36.50	36.50

734

<sup>A</sup>Al(OH)<sub>3</sub> and Fe(OH)<sub>3</sub> allowed to precipitate using the parameters given in the main text.

735

<sup>B</sup>Adjusted to maintain charge balance across the pH range simulated.

736



**Table 2. Field datasets used for WHAM/Model VII testing**

Metal	Measurement method	<i>n</i>	Code	Reference
Al	Cation exchange column + speciation	55	Al-01	[28]
	Cation exchange column + speciation	180	Al-02	[28]
	Cation exchange column + speciation	167	Al-03	[28]
Co	CLE-DPCSV <sup>A</sup>	7	Co-01	[7]
Ni	IET <sup>B</sup>	3	Ni-01	[17]
	DMT <sup>C</sup>	3	Ni-02	[16]
	DMT	7	Ni-03	[6]
	DMT	35	Ni-04	[32]
	DMT	6	Ni-05	[35]
Cu	CLE-AdCSV <sup>D</sup>	2	Cu-01	[48]
	CLE-DPCSV	14	Cu-02	[8]
	CLE-DPCSV	38	Cu-03	[9]
	CLE-CSV <sup>E</sup>	5	Cu-04	[10]
	CLE-CSV	15	Cu-05	[11]
	PLM <sup>F</sup>	2	Cu-06a	[16]
	DMT	3	Cu-06b	[16]
	DMT	7	Cu-07	[6]
	DMT	35	Cu-08	[32]
	IET	10	Cu-09	[49]
	Zn	CLE-DPASV <sup>G</sup>	4	Zn-01
CLE-DPASV		12	Zn-02	[8]
CLE-DPASV		6	Zn-03	[12]
DMT		5	Zn-04	[6]
DMT		34	Zn-05	[32]
IET		24	Zn-06	[49]
Cd	CLE-AdCSV	4	Cd-01	[48]
	CLE-DPASV	11	Cd-02	[13]
	PLM	3	Cd-03a	[16]
	DMT	2	Cd-03b	[16]
	DMT	6	Cd-04	[6]
	DMT	35	Cd-05	[32]
	IET	24	Cd-06	[49]
Pb	CLE-DPCSV	28	Pb-01	[10]
	PLM	2	Pb-02a	[16]
	DMT	3	Pb-02b	[16]
	DMT	7	Pb-03	[6]
	DMT	35	Pb-04	[32]

738 <sup>A</sup>Competitive ligand exchange–differential pulse cathodic stripping voltammetry.

739 <sup>B</sup>Ion exchange column method.

740 <sup>C</sup>Donnan membrane technique.

741 <sup>D</sup>Competitive ligand exchange–adsorptive cathodic stripping voltammetry.

742 <sup>E</sup>Competitive ligand exchange–cathodic stripping voltammetry.

743 <sup>F</sup>Permeation liquid membrane.

744 <sup>G</sup>Competitive ligand exchange–differential pulse anodic stripping voltammetry.

745

746

**Table 3. Uncertainties in WHAM/Model VII inputs used in this study**

Variable	Uncertainty type	$\sigma_i$ or $p_i$
Input variables		
Temperature (K)	Absolute	1
$p\text{CO}_2$	Relative	0.025
pH	Absolute	0.05
Colloidal fulvic acid ( $\text{g L}^{-1}$ )	Relative	0.09
Solute concentrations <sup>A</sup> (M)	Relative	0.025
Parameters – Model VII		
$\log K_{\text{MA}}$	Absolute	0.3
Parameters – iron(III) oxide		
$pK_{\text{MH,oxide}}$	Absolute	0.3
Solution speciation		
$\log K_{\text{SO,Fe(OH)3}}$	Absolute	0.7
$\log K_{\text{SO,Al(OH)3}}$	Absolute	0.7

747 <sup>A</sup>Solutes comprise dissolved metals, major ions and alkalinity.

748

749 **Table 4. Bias, error (root mean square error, RMSE) and variability in WHAM predictions of**  
750 **field speciation of Al, Co, Ni, Cu, Zn and Cd, and numbers of observations falling within the**  
751 **interquartile range 2.5–97.5 % of the predictions**

752 For variability ( $Q_{16-84}$ ), the interquartile range of the predictions of log free metal ion is 16–84 %.  
753 Input variables include uncertainty in  $F_{\text{FADOC}}$ . For observations within  $Q_{2.5-97.5}$ , the interquartile range  
754 of the predictions of log free metal ion is 2.5–97.5 %. Bold entries refer to bias, error and variability  
755 in predictions for each metal as a whole.

Metal	Dataset	$n_{\text{obs}}$	Mean observed $\log[M^{z+}]$	Mean predicted $\log[M^{z+}]$	Bias	RMSE	Input variables	Variability ( $Q_{16-84}$ ) Parameters	All	Observations within $Q_{2.5-97.5}$
Al	Al-01	55	-6.03	-6.23	0.20	0.29	0.68	0.44	0.82	55
	Al-02	180	-7.69	-7.84	0.16	0.29	0.56	0.56	0.82	173
	Al-03	167	-6.01	-6.73	0.72	0.81	0.60	0.64	0.88	127
	<b>All Al</b>	<b>402</b>	<b>-6.76</b>	<b>-7.14</b>	<b>0.38</b>	<b>0.54</b>	<b>0.60</b>	<b>0.58</b>	<b>0.84</b>	<b>355</b>
Co	Co-01	7	-9.74	-9.36	0.33	0.40	0.14	0.0024	0.14	0
Ni	Ni-01	3	-6.65	-6.24	0.41	0.46	0.14	0.0086	0.15	0
	Ni-02	3	-9.54	-9.24	0.30	0.46	0.18	0.058	0.19	1
	Ni-03	7	-9.35	-8.48	0.86	0.95	0.18	0.030	0.19	0
	Ni-04	35	-8.75	-8.00	0.75	0.92	0.16	0.052	0.17	1
	Ni-05	6	-8.01	-7.89	0.12	0.30	0.18	0.084	0.20	2
	<b>All Ni</b>	<b>54</b>	<b>-8.67</b>	<b>-8.02</b>	<b>0.65</b>	<b>0.83</b>	<b>0.16</b>	<b>0.050</b>	<b>0.18</b>	<b>4</b>
Cu	Cu-01	2	-8.86	-10.71	-1.84	1.84	0.44	0.56	0.76	0
	Cu-02	14	-13.62	-10.29	3.34	3.39	0.44	0.46	0.62	0
	Cu-03	39	-13.44	-10.89	2.55	2.73	0.40	0.62	0.76	4
	Cu-04	5	-14.82	-10.62	4.30	4.30	0.32	0.76	0.84	0
	Cu-05	15	-15.05	-11.47	3.58	3.97	0.46	0.64	0.80	0
	Cu-06a	3	-10.37	-11.71	-1.33	1.48	0.38	0.62	0.68	1
	Cu-06b	3	-10.36	-11.71	-1.34	1.53	0.38	0.62	0.68	1
	Cu-07	7	-10.46	-10.90	-0.44	1.19	0.44	0.58	0.76	2
	Cu-08	35	-10.19	-10.11	0.078	1.19	0.38	0.48	0.64	12
	Cu-09	10	-8.02	-9.47	-1.44	1.76	0.48	0.58	0.78	3
<b>All Cu</b>	<b>133</b>	<b>-12.00</b>	<b>-10.87</b>	<b>1.76</b>	<b>2.62</b>	<b>0.40</b>	<b>0.54</b>	<b>0.68</b>	<b>23</b>	
Zn	Zn-01	4	-7.15	-7.42	-0.27	0.57	0.26	0.28	0.40	4
	Zn-02	12	-8.31	-7.52	0.80	0.84	0.15	0.046	0.15	0
	Zn-03	5	-8.68	-8.28	0.40	0.41	0.15	0.054	0.16	0
	Zn-04	4	-8.00	-7.27	0.73	0.84	0.18	0.11	0.22	1
	Zn-05	34	-6.44	-6.59	0.15	0.33	0.21	0.15	0.28	16
	Zn-06	25	-7.44	-8.20	-0.76	0.84	0.30	0.34	0.45	2
	<b>All Zn</b>	<b>84</b>	<b>-7.26</b>	<b>-7.38</b>	<b>-0.12</b>	<b>0.65</b>	<b>0.22</b>	<b>0.19</b>	<b>0.30</b>	<b>23</b>
Cd	Cd-01	4	-9.61	-8.91	0.69	0.81	0.24	0.19	0.30	3
	Cd-02	11	-12.00	-10.85	1.16	1.26	0.22	0.19	0.28	2
	Cd-03a	3	-11.22	-10.57	0.65	1.10	0.20	0.13	0.26	0
	Cd-03b	2	-11.61	-10.64	0.97	1.12	0.20	0.13	0.26	0
	Cd-04	5	-11.19	-10.00	1.19	1.27	0.17	0.060	0.18	0
	Cd-05	35	-9.29	-9.11	0.19	0.33	0.18	0.092	0.22	20
	Cd-06	25	-9.54	-9.90	-0.36	0.42	0.28	0.26	0.38	11
<b>All Cd</b>	<b>85</b>	<b>-9.96</b>	<b>-9.71</b>	<b>0.27</b>	<b>0.71</b>	<b>0.22</b>	<b>0.16</b>	<b>0.28</b>	<b>36</b>	

756  
757

758 **Table 5. Bias, error (root mean square error, RMSE) and variability in WHAM predictions of**  
759 **field speciation of Pb, and numbers of observations falling within the interquartile range 2.5–**  
760 **97.5 % of the predictions**

761 For variability ( $Q_{16-84}$ ), the interquartile range of the predictions of log free metal ion is 16–84 %.  
762 Input variables include uncertainty in  $F_{\text{FADOC}}$ . For observations within  $Q_{2.5-97.5}$ , the interquartile range  
763 of the predictions of log free metal ion is 2.5–97.5 %. Bold entries refer to bias, error and variability  
764 in predictions for each metal as a whole.

Dataset	$n_{\text{obs}}$	Mean observed $\log[M^{2+}]$	Mean predicted $\log[M^{2+}]$	Bias	RMSE	Input variables	Variability ( $Q_{16-84}$ ) Parameters	All	Observations within $Q_{2.5-97.5}$
Not considering binding by iron(III) oxide									
Pb-01	28	-13.20	-10.56	2.64	2.83	0.28	0.36	0.42	1
Pb-02a	3	-11.49	-10.70	-0.53	0.53	0.22	0.16	0.56	0
Pb-02b	3	-11.30	-10.70	-0.72	0.72	0.22	0.16	0.56	0
Pb-03	7	-11.90	-11.40	0.50	0.93	0.26	0.20	0.32	1
Pb-04	35	-9.81	-9.38	0.46	1.12	0.34	0.36	0.48	5
<b>All Pb</b>	<b>76</b>	<b>-11.38</b>	<b>-10.11</b>	<b>1.17</b>	<b>1.69</b>	<b>0.30</b>	<b>0.33</b>	<b>0.45</b>	<b>7</b>
Considering binding by iron(III) oxide									
Pb-01	28	-13.20	-11.48	1.72	1.96	0.26	0.20	0.54	2
Pb-02a	3	-11.49	-12.51	-1.02	1.09	0.20	0.22	0.30	0
Pb-02b	3	-11.30	-12.51	-1.21	1.29	0.20	0.22	0.30	0
Pb-03	7	-11.90	-11.77	0.13	0.85	0.22	0.22	0.26	1
Pb-04	35	-9.81	-9.50	0.31	1.14	0.26	0.35	0.46	6
<b>All Pb</b>	<b>76</b>	<b>-11.38</b>	<b>-10.68</b>	<b>0.70</b>	<b>1.48</b>	<b>0.26</b>	<b>0.28</b>	<b>0.46</b>	<b>9</b>

765

766

767 **Table 6. Bias and scatter (root mean squared error, RMSE) in WHAM predictions of field**  
768 **speciation of Cu, Zn, Cd and Pb, for all free ion observations and for observations not obtained**  
769 **using voltammetry**

Parameter	Copper		Zinc		Cadmium		Lead	
	All	Not including voltammetry	All	Not including voltammetry	All	Not including voltammetry	All	Not including voltammetry
$n_{\text{obs}}$	133	58	84	63	85	70	76	48
Mean observed $\log[M^{z+}]$	-12.00	-9.87	-7.26	-6.94	-9.96	-9.66	-11.38	-10.31
Mean predicted $\log[M^{z+}]$	-10.87	-10.26	-7.38	-7.27	-9.71	-9.56	-10.68	-10.21
Bias	1.76	-0.39	-0.12	-0.17	0.27	0.11	0.70	0.11
RMSE	2.62	1.32	0.65	0.56	0.71	0.48	1.48	1.10

770 **Fig. 1.** Distribution of estimated dissolved organic carbon (DOC) ‘activity’, from Bryan and coworkers.<sup>[26]</sup>

771 The DOC ‘activity’ ( $F_{\text{FADOC}}$ ) is the ratio of model-optimised fulvic acid to measured DOC. The dashed lines  
772 represent the mean, mean + 1 standard deviation and mean – 1 standard deviation of  $\log F_{\text{FADOC}}$ . The Anderson–  
773 Darling test indicated no significant departure from normality at a significance level of  $P = 0.05$ .

774 **Fig. 2.** Theoretical calculations of variability in free ion concentrations of Al: calculated free concentrations  
775 and  $Q_{16-84}$  ranges for the chemical conditions given in Table 3 and pH 5.0 (closed symbols), pH 6.0 (open  
776 symbols), for four uncertainty scenarios. 1 = uncertainty in  $F_{\text{FADOC}}$  only, 2 = uncertainty in  $F_{\text{FADOC}}$  and input  
777 variables, 3 = uncertainty in parameters only, 4 = uncertainty in  $F_{\text{FADOC}}$ , input variables and parameters together.

778 **Fig. 3.** Theoretical calculations of variability in free ion concentrations of Co, Ni, Cu, Zn, Cd and Pb:  
779 calculated free concentrations and  $Q_{16-84}$  ranges for the chemical conditions given in Table 3 and pH 7.0, for  
780 four uncertainty scenarios. 1 = uncertainty in  $F_{\text{FADOC}}$  only, 2 = uncertainty in  $F_{\text{FADOC}}$  and input variables, 3 =  
781 uncertainty in parameters only, 4 = uncertainty in  $F_{\text{FADOC}}$ , input variables and parameters together.

782 **Fig. 4.** Comparison of  $\text{Pb}^{2+}$  concentrations calculated assuming iron(III) oxide to be an active binding phase  
783 with concentrations calculated assuming iron(III) oxide to be inert with respect to ion binding.  $\text{FeOx} = \text{iron(III)}$   
784 oxide.

785 **Fig. 5.** Comparison of  $\text{Al}^{3+}$  concentrations calculated by speciation of inorganic monomeric Al and by  
786 speciation of total monomeric Al, for all Al datasets. Error bars indicate the  $Q_{16-84}$  range predicted by  
787 WHAM/Model VII.

788 **Fig. 6.** Comparison of observed  $\text{Co}^{2+}$  concentrations with predictions of WHAM/Model VII, for dataset Co-  
789 01. Error bars indicate the  $Q_{16-84}$  range predicted by WHAM/Model VII.

790 **Fig. 7.** Comparison of observed  $\text{Ni}^{2+}$  concentrations with predictions of WHAM/Model VII, for all Ni  
791 datasets. Vertical error bars indicate the  $Q_{16-84}$  range predicted by WHAM/Model VII, horizontal error bars  
792 represent  $\pm 1$  standard deviation of measurements, where quoted.

793 **Fig. 8.** Comparison of observed  $\text{Cu}^{2+}$  concentrations with predictions of WHAM/Model VII, for  
794 measurements made by voltammetry (top), by Donnan membrane technique (DMT) (middle) and by Permeation  
795 liquid membrane (PLM) or ion exchange column method (IET) (bottom). Vertical error bars indicate the  $Q_{16-84}$   
796 range predicted by WHAM/Model VII, horizontal error bars represent  $\pm 1$  standard deviation of measurements,  
797 where quoted. CLE-AdCSV: competitive ligand exchange adsorptive cathodic stripping voltammetry; CLE-

798 DPCSV: competitive ligand exchange differential pulse cathodic stripping voltammetry; CLE-CSV: competitive  
799 ligand exchange cathodic stripping voltammetry.

800 **Fig. 9.** Comparison of observed  $Zn^{2+}$  concentrations with predictions of WHAM/Model VII, for measurements  
801 made by voltammetry (top) and by Donnan membrane technique (DMT) and ion exchange column method  
802 (IET) (bottom). Vertical error bars indicate the  $Q_{16-84}$  range predicted by WHAM/Model VII, horizontal error  
803 bars represent  $\pm 1$  standard deviation of measurements, where quoted. CLE-DPASV: competitive ligand  
804 exchange differential pulse anodic stripping voltammetry.

805 **Fig. 10.** Comparison of observed  $Cd^{2+}$  concentrations with predictions of WHAM/Model VII, for  
806 measurements made by voltammetry, permeation liquid membrane (PLM), and ion exchange column method  
807 (IET) (top), and by Donnan membrane technique (DMT) (bottom). Vertical error bars indicate the  $Q_{16-84}$  range  
808 predicted by WHAM/Model VII, horizontal error bars represent  $\pm 1$  standard deviation of measurements, where  
809 quoted. CLE-AdCSV: competitive ligand exchange adsorptive cathodic stripping voltammetry; CLE-DPCSV:  
810 competitive ligand exchange differential pulse cathodic stripping voltammetry.

811 **Fig. 11.** Comparison of observed  $Pb^{2+}$  concentrations with predictions of WHAM/Model VII, for  
812 measurements made by voltammetry and permeation liquid membrane (PLM) (top), and by Donnan membrane  
813 technique (DMT) (bottom). Vertical error bars indicate the  $Q_{16-84}$  range predicted by WHAM/Model VII,  
814 horizontal error bars represent  $\pm 1$  standard deviation of measurements, where quoted. CLE-DPCSV:  
815 Competitive ligand exchange differential pulse cathodic stripping voltammetry.  
816